

A simple design method for broadband
planar antennasRongLin Li, Zhenkai Yang, Yang Zhang and Yuehui Cui 

School of Electronic and Information Engineering, South China University of Technology, Guangzhou 510641, China

Research Paper

Cite this article: Li R, Yang Z, Zhang Y, Cui Y (2023). A simple design method for broadband planar antennas. *International Journal of Microwave and Wireless Technologies* **15**, 1781–1788. <https://doi.org/10.1017/S1759078723000478>

Received: 1 January 2023

Revised: 30 March 2023

Accepted: 30 March 2023

Keywords:

bandwidth enhancement; base station; broadband planar antenna; design method; dual polarization

Corresponding author: Yuehui Cui;Email: eeyhcu@scut.edu.cn**Abstract**

A simple process for the design of broadband planar antennas is presented for base station applications. The process is based on a square patch above a ground plane. Only three geometric parameters are involved in the design of a dual-polarized broadband planar antenna, including the width (W_s) of the square patch, a trimming angle (θ) of the square, and the height (H) of the patch above the ground plane. By adjusting the critical parameters θ and H , an impedance bandwidth of 50% for return loss (RL) > 15 dB is achieved with an isolation of higher than 35 dB. The bandwidth of the broadband planar antenna is enhanced to 67% by etching four Γ slots on the square patch. The operating mechanisms of these broadband antennas are analyzed and verified by simulation and experiment.

Introduction

Antennas with enhanced wide bandwidth are widely needed for modern mobile communication systems [1–16]. There is a strong requirement for base station antennas to have stable radiation patterns with desired beamwidth, well matched impedance, enough high gain, and good isolation over the operation bandwidth. Therefore, dual linearly polarized dipole antennas have been widely employed for base station applications. Most of dual-polarized antennas are developed based on two orthogonal dipoles [2–16]. Many geometric parameters are involved in the optimization for a broadband operation. Seven or eight geometric parameters (not including the ground plane or the reflector) are involved for a relative bandwidth of ~45% for return loss (RL) > 15 dB or voltage standing wave ratio (VSWR) < 1.5 in [2–4]. The dual-polarized antennas developed in [5–8] have about 20 geometric parameters for a bandwidth of ~55% for RL > 15 dB or VSWR < 1.5. Different numbers of geometric parameters from 10 to 34 are involved for the bandwidth-enhanced broadband antennas in [9–16] to realize a bandwidth of ~65% for RL > 15 dB or VSWR < 1.5.

In this work, we propose a simple design method for broadband dual-polarized planar base station antennas. The design process is based on a square patch. Only two critical geometric parameters for a broadband antenna are adjusted to achieve a bandwidth of 50% for RL > 15 dB, including the trimming angle of the square patch and the height of the patch above a ground plane. By etching four Γ slots on the square patch and optimizing five geometric parameters, the bandwidth of the broadband antenna is enhanced to 67% for RL > 15 dB. Both broadband antennas feature a simple planar configuration and stable radiation pattern. The design method for broadband planar antennas is described in the Section “Design method and analysis” and verified in the Section “Realization and verification.” The enhancement of bandwidth of the broadband antenna is described in the Section “Bandwidth enhancement.”

Design method and analysis

The design procedure for a broadband dual-polarized antenna starts from a square metal patch of width W_s , as illustrated in Fig. 1. The width W_s depends on the center frequency (f_0) of the operation frequency band. To construct a dual-polarized antenna, the square patch is trimmed into two dipoles, i.e., the +45° polarized dipole fed by Port 1 and the -45° polarized dipole fed by Port 2, along its center with a trimming angle θ . The trimmed square patch is placed above a ground plane (or a reflector) with a height H for unidirectional radiation patterns.

When the +45° polarized dipole is driven by an ideal voltage source alone (removing the -45° polarized dipole and the ground plane), a resonance is created at f_r , as shown in Fig. 2. The square width is about a quarter-wavelength ($\lambda_r/4$) at f_r . As the -45° polarized

© The Author(s), 2023. Published by Cambridge University Press in association with the European Microwave Association. This is an Open Access article, distributed under the terms of the Creative Commons Attribution-ShareAlike licence (<http://creativecommons.org/licenses/by-sa/4.0>), which permits re-use, distribution, and reproduction in any medium, provided the same Creative Commons licence is used to distribute the re-used or adapted article and the original article is properly cited.

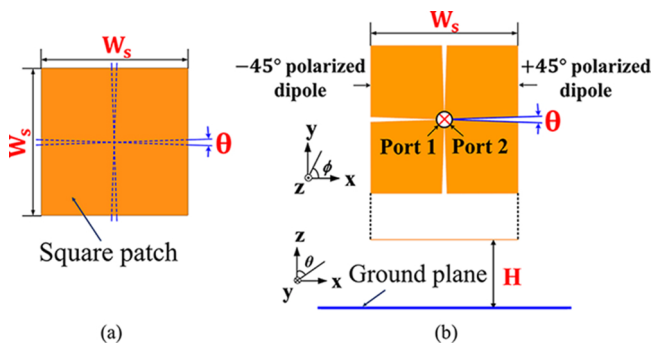


Figure 1. Development of a broadband dual-polarized antenna based on a square patch: (a) square patch and (b) dual-polarized antenna.

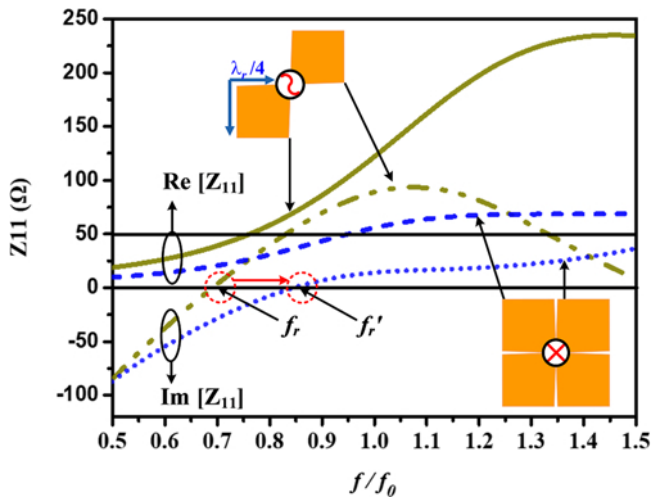


Figure 2. A resonance created by the +45° polarized dipole alone compared to the resonance with the -45° polarized dipole moved in.

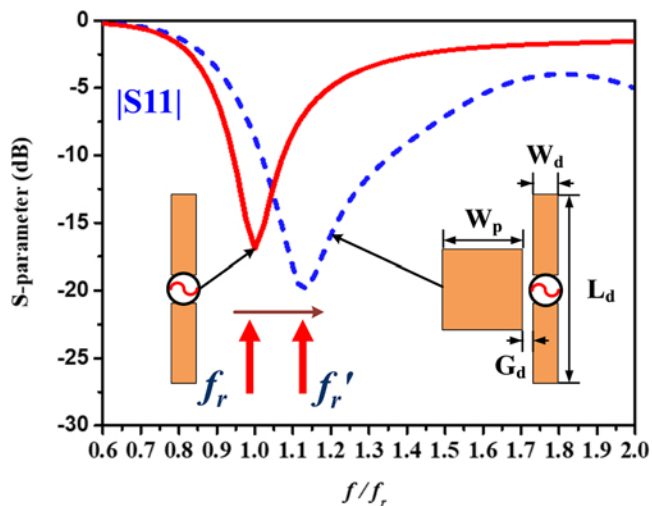


Figure 3. The resonant frequency f_r of a planar dipole shifted up to f_r' as a parasitic square patch is introduced nearby ($L_d = 0.48\lambda_r$, $W_d = 0.05\lambda_r$, $W_p = 0.24\lambda_r$, and $G_d = 0.02\lambda_r$).

dipole is moved in, the resonant frequency f_r moves to a higher resonant frequency f_r' . Note that there is only one resonance for the dual-polarized antenna without the ground plane.

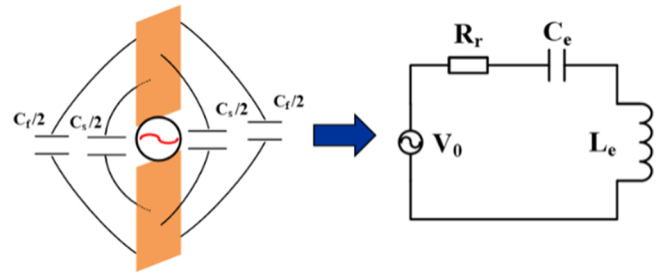


Figure 4. The equivalent circuit for the resonant frequency of a dipole.

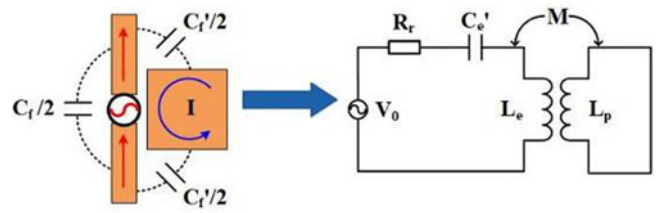


Figure 5. The equivalent circuit for the resonant frequency of a dipole nearby a parasitic square patch.

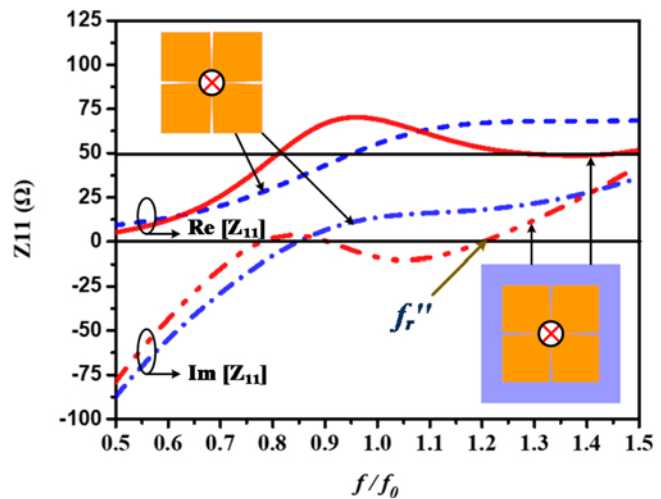


Figure 6. A new resonance generated at f_r'' for the dual-polarized antenna above a ground plane.

The shift of resonant frequency from f_r up to f_r' is due to the mutual coupling between the $\pm 45^\circ$ polarized dipoles. Consider an isolated planar dipole whose resonant frequency is f_r , see Fig. 3. When a parasitic square patch is introduced nearby, the resonant frequency of the dipole is shifted up to f_r' , as does the +45° polarized dipole with the -45° polarized dipole moved in. The mechanism for the frequency upshifting can be explained by an equivalent-circuit analysis. The inductance of the dipole at f_r is assumed to be L_e , while its capacitance C_e is

$$C_e = C_s + C_f \approx C_s, \tag{1}$$

where C_s and C_f are the surface-to-surface and the edge-to-edge capacitances, respectively, between the two arms of the planar dipole, as sketched in Fig. 4. Since the edge-to-edge capacitance C_f is much smaller than the surface-to-surface capacitance C_s , C_f is negligible for the resonance. The resonant frequency f_r of the dipole can be expressed as

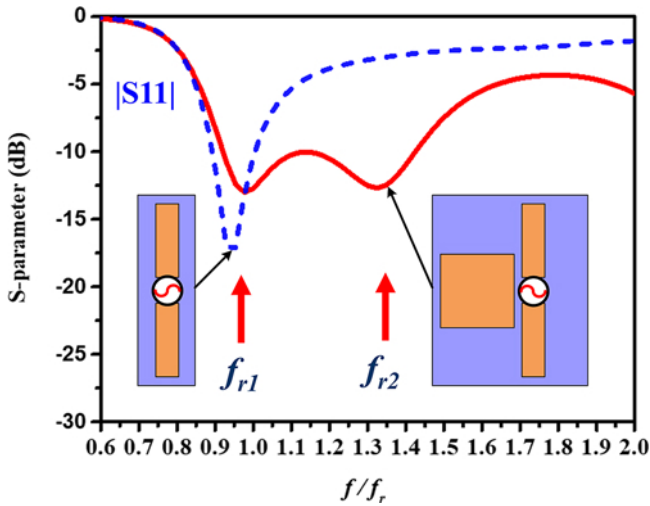


Figure 7. Two resonances of a dipole created at f_{r1} and f_{r2} by a parasitic element and a ground plane.

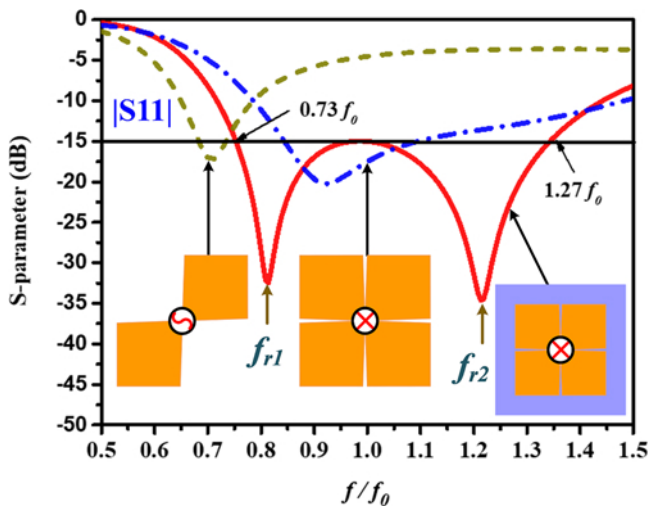


Figure 8. Evolution of a dual-polarized antenna from the $+45^\circ$ polarized dipole to the broadband antenna.

$$f_r = \frac{1}{2\pi\sqrt{L_e C_e}} \tag{2}$$

When a parasitic square patch is placed nearby the planar dipole, the capacitance of the dipole becomes C_e' :

$$C_e' = C_s + C_f/2 + C_f' \approx C_s, \tag{3}$$

where C_f' is the capacitance between the edges of the dipole and the square patch, as depicted in Fig. 5. C_f' is also negligible; thus, $C_e' \cong C_e$. Due to the mutual coupling (mutual inductance M) between the dipole and the square patch, the inductance L_e' of the dipole nearby the square patch decreases as

$$L_e' = L_e - \frac{M^2}{L_p}, \downarrow \tag{4}$$

where L_p is the self-inductance of the square patch. As a result, the resonant frequency f_r' of the dipole with a parasitic element increases as

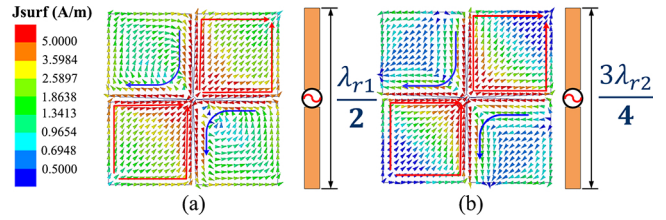


Figure 9. Current distributions on the dual-polarized broadband antenna at (a) f_{r1} and (b) f_{r2} .

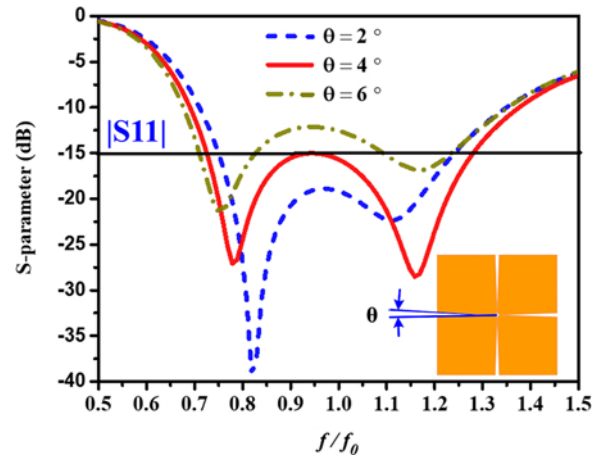


Figure 10. The effect of the trimming angle θ on the S-parameter $|S_{11}|$ of the broadband antenna.

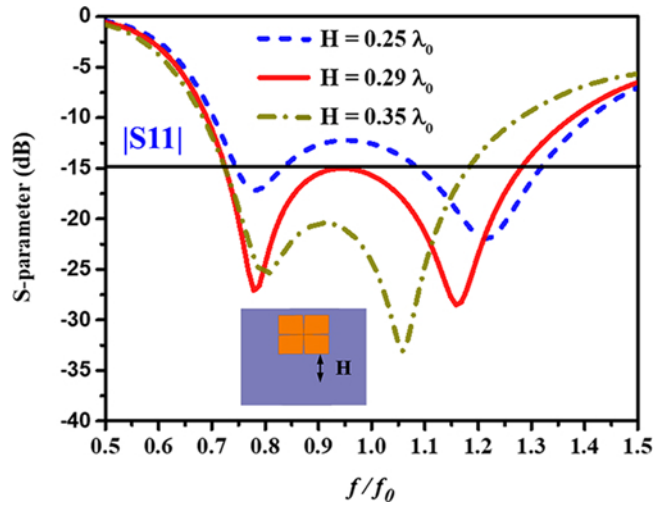


Figure 11. The effect of the height H on the S-parameter $|S_{11}|$ of the broadband antenna.

$$f_r' = \frac{1}{2\pi\sqrt{L_e' C_e'}}, \uparrow \tag{5}$$

The -45° polarized dipole plays the same role for the resonance of the $+45^\circ$ polarized dipole as does the square patch for the planar dipole. It is predicted that the resonance length of a dual-polarized dipole antenna will be longer than half the wavelength due to the mutual coupling.

Only the dipole with a parasitic element above a ground plane can create two resonances at f_{r1} and f_{r2} . A combination of the two

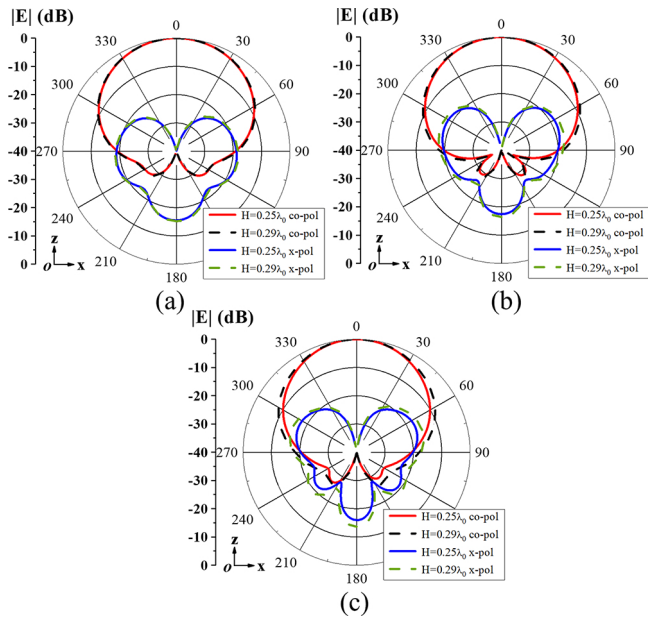


Figure 12. Radiation patterns of the broadband antenna for +45° polarization at (a) $f = 0.73f_0$, (b) $f = f_0$, and (c) $f = 1.27f_0$.

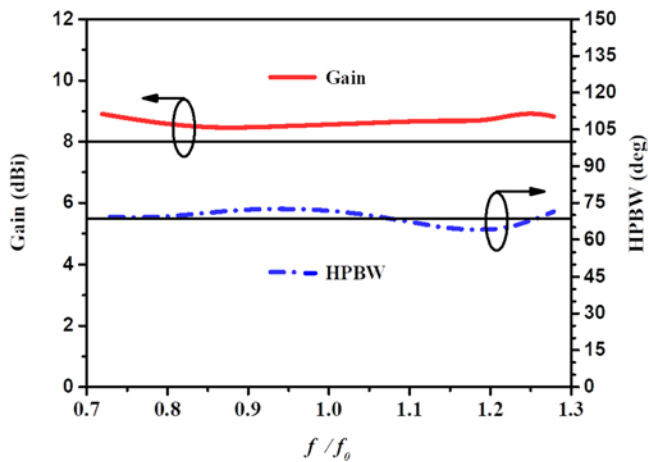


Figure 13. Gain and HPBW of the broadband antenna.

resonances leads to a broadband operation. Therefore, the mutual couplings between the +45° and the -45° polarized dipoles and between the ±45° polarized dipoles and the ground plane play a critical role for the broadband performance. The trimming angle θ is related to the coupling between the +45° and the -45° polarized dipoles, while the height H is associated with the coupling between the ±45° polarized dipoles and the ground plane. By adjusting the critical geometric parameters θ and H , a broadband dual-polarized antenna can be obtained.

When the dual-polarized antenna is placed above the ground plane, a new resonance at f_r'' is generated, as exhibited in Fig. 6. This resonance is attributed to the mutual coupling between the dual-polarized antenna and the ground plane. Note that an isolated dipole above a ground plane will not generate a new resonance, as demonstrated in Fig. 7.

Fig. 8 demonstrates the evolution of a dual-polarized antenna from the +45° polarized dipole alone to ±45° polarized dipoles without the ground plane and eventually to the broadband

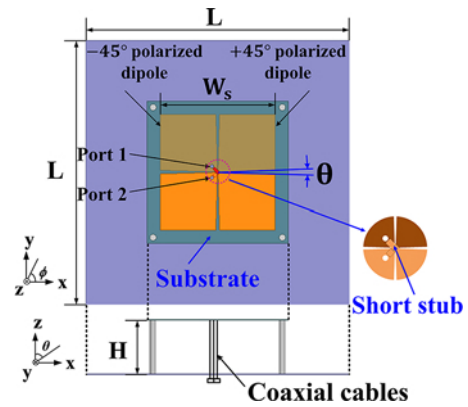


Figure 14. Broadband antenna realized on a thin substrate ($W_s = 53$ mm, $\theta = 4^\circ$, $H = 36$ mm, and $L = 150$ mm).

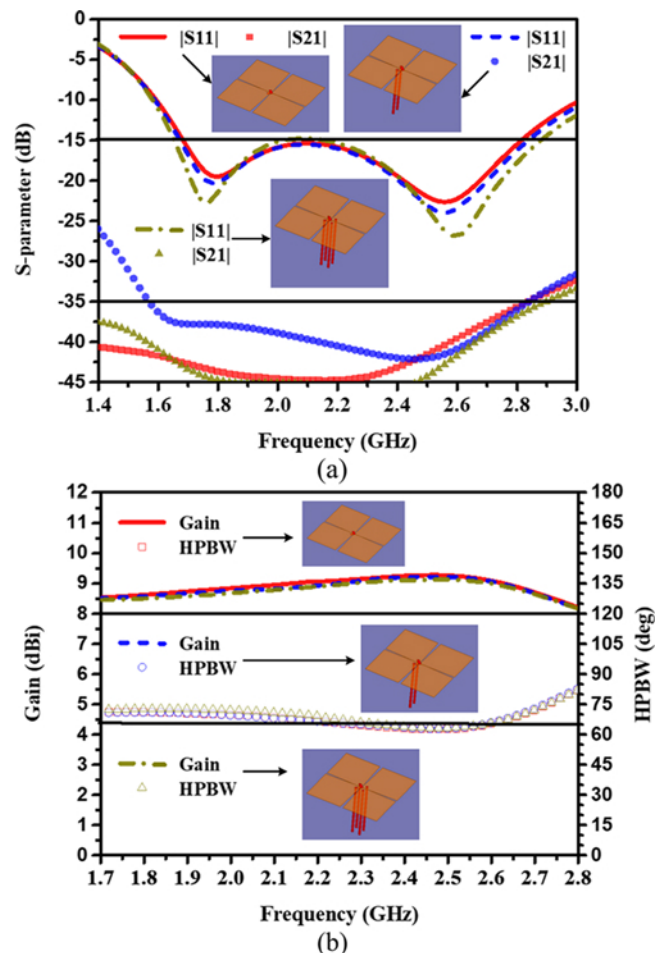


Figure 15. The effect of the coaxial cables on the performance of the broadband antenna: (a) S-parameters and (b) gain and HPBW.

antenna. Two resonances at f_{r1} and f_{r2} are observed for the broadband antenna. A bandwidth of 54% for $RL > 15$ dB is obtained. The broadband antenna operates as a half-wave dipole at f_{r1} and a three-quarter-wavelength dipole at f_{r2} as verified by the current distributions displayed in Fig. 9.

The broadband antenna involves three geometric parameters, i.e., the width W_s of the square patch, the trimming angle θ , and

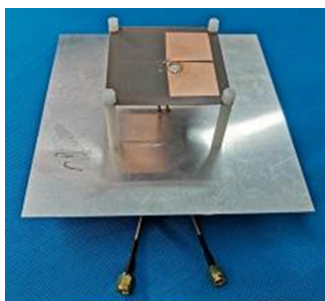


Figure 16. A prototype of the realized broadband antenna.

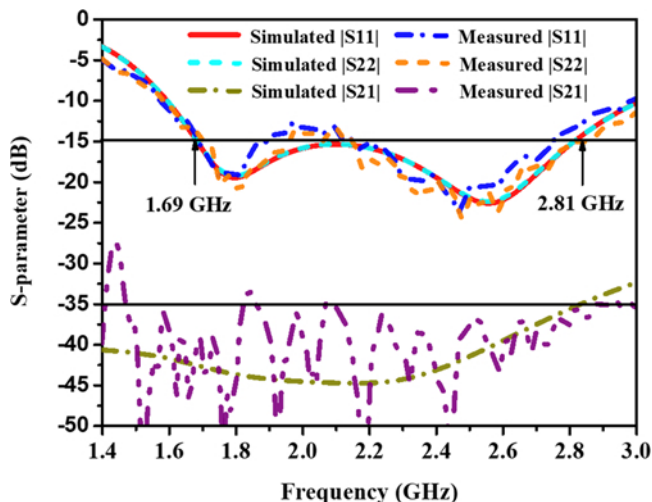


Figure 17. Simulated and measured S-parameters of the broadband antenna.

the height H above the ground plane. The square width W_s is decided by the operation frequency band, which is found to be $W_s = 0.414\lambda_0$, where λ_0 is the wavelength in free space at f_0 . The critical geometric parameters θ and H are adjusted for a broadband operation. Fig. 10 shows the effect of trimming angle θ on the S-parameter $|S_{11}|$ of the broadband antenna. The widest bandwidth is obtained when $\theta = 4^\circ$ for $RL > 15$ dB. The effect of the height H on the S-parameter of the broadband antenna is plotted in Fig. 11. The widest bandwidth is found when $H = 0.29\lambda_0$ for $RL > 15$ dB. Stable radiation patterns are observed from $f = 0.73f_0$ to $f = 1.27f_0$ as displayed in Fig. 12. The antenna gain is about 8.5 dBi and the HPBW is $68 \pm 5^\circ$ as demonstrated in Fig. 13.

Realization and verification

The broadband dual-polarized antenna is realized on a thin substrate (Taconic TLY-5, $\epsilon_r = 2.2$, thickness = 0.5 mm) for the 2 GHz band (1.7–2.7 GHz). The configuration of the realized broadband antenna is illustrated in Fig. 14. Three geometric parameters associated with the broadband antenna are found to be $W_s = 53$ mm, $\theta = 4^\circ$, and $H = 36$ mm. One arm of each dipole (the $+45^\circ / -45^\circ$ polarized dipole) is printed on one side of the substrate while the other arm is etched on the other side of the substrate. The voltage source is simply realized with a shot stub. Each stub with one arm of the dipole serves as a microstrip line, which can be connected to the coaxial cable. The width of the stub is determined to be 1.6 mm for a characteristic impedance of 50 Ω . Each stub extends a short length from the dipole arms in order

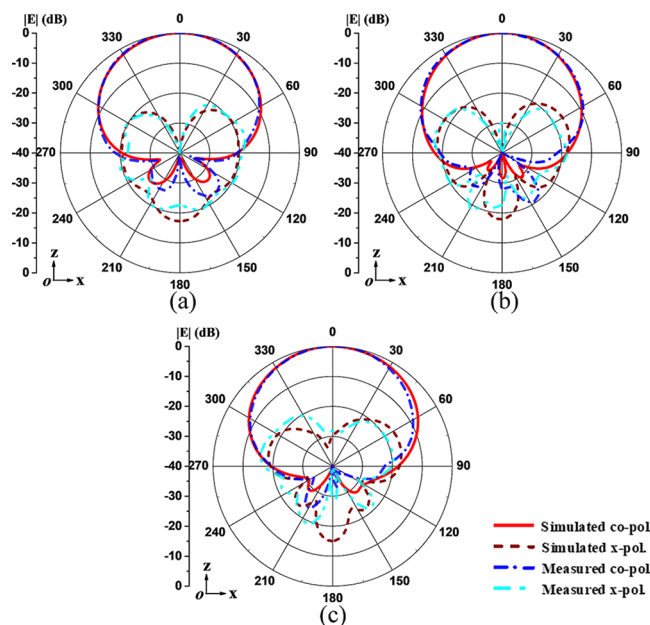


Figure 18. Radiation patterns of the broadband antenna simulated and measured for $+45^\circ$ polarization at (a) 1.7 GHz, (b) 2.2 GHz, and (c) 2.8 GHz.

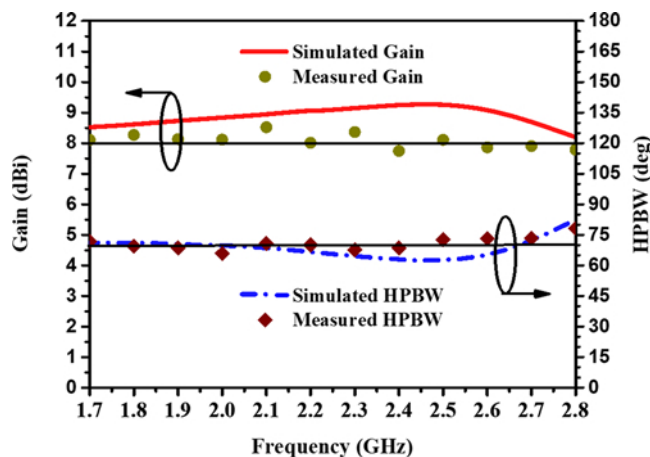


Figure 19. Gain and HPBW of the broadband antenna.

to separate the two feeding points for the dual-polarized antenna from being overlapped. Each dipole is fed by a coaxial cable whose outer conductor is soldered to an arm while its inner conductor is connected to the other arm through a short stub. The feeding coaxial cables have little effect on the performance of the broadband antenna. Fig. 15 shows (A) the S-parameters and (B) gain and HPBW when the broadband antenna is fed with an ideal voltage source, with two coaxial cables or with two coaxial cables plus two supporting metal poles. Little differences can be seen.

A prototype of the realized broadband antenna is pictured in Fig. 16. The simulated and measured S-parameters are compared in Fig. 17; good agreement is observed. The measured bandwidth for $|S_{11}|$ and $|S_{22}| < -15$ dB (or $RL > 15$) is about 50%, covering the frequency band 1.69–2.81 GHz for 2G/3G/4G base stations. The measured isolation ($-|S_{21}|$ in dB) is higher than 35 dB. The radiation patterns simulated and measured for $+45^\circ$ polarization at 1.7, 2.2, and 2.8 GHz are plotted in Fig. 18; stable radiation patterns are observed from 1.7 to 2.8 GHz. The gain and the HPBW of

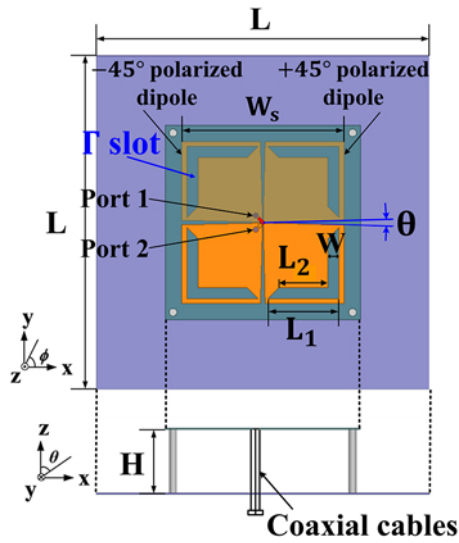


Figure 20. Bandwidth-enhanced broadband antenna with four Γ slots ($W_s = 63$ mm, $\theta = 3^\circ$, $H = 45$ mm, $L_1 = 28$ mm, $L_2 = 19$ mm, $w = 4.3$ mm, and $L = 160$ mm).

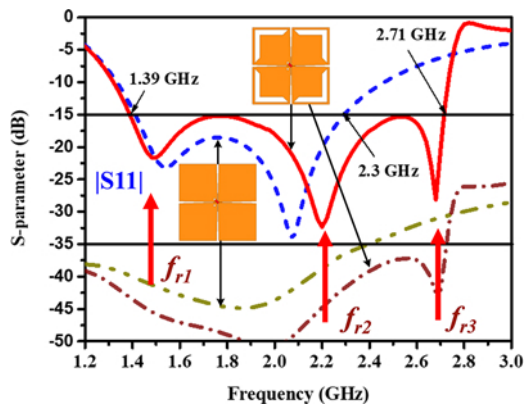


Figure 21. The third resonance at f_{r3} created by the Γ slots.

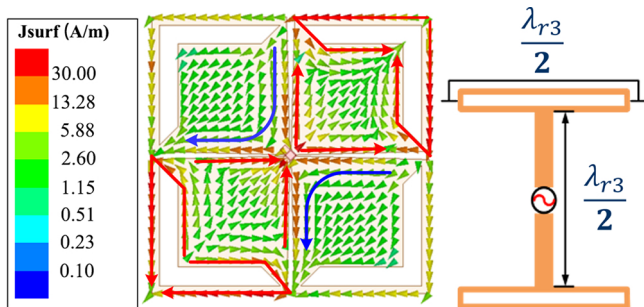


Figure 22. Current distribution on the bandwidth-enhanced broadband antenna at f_{r3} .

the broadband antenna are presented in Fig. 19. The antenna gain realized is about 8 ± 0.5 dBi and the HPBW is $70 \pm 5^\circ$.

Bandwidth Enhancement

The bandwidth of the broadband antenna can be enhanced by introducing a Γ slot on every arm of the dipoles, as illustrated in

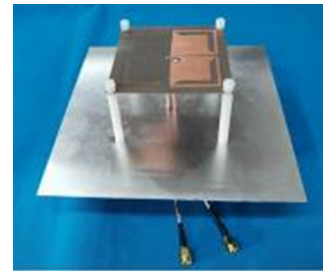


Figure 23. A prototype of the bandwidth-enhanced broadband antenna.

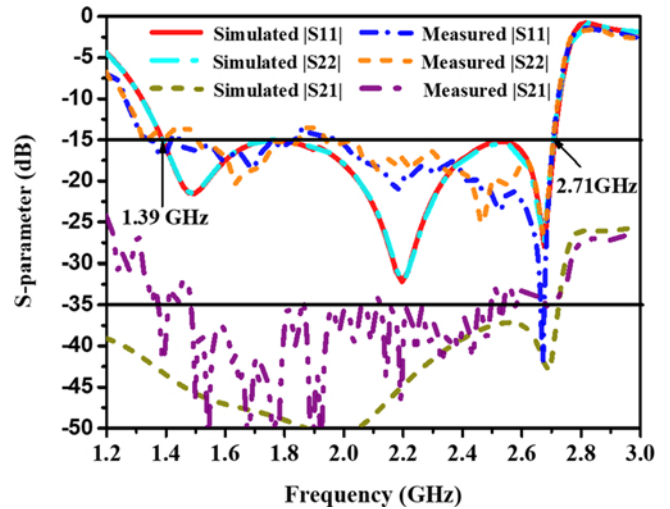


Figure 24. Measured and simulated S-parameters of the bandwidth-enhanced broadband antenna.

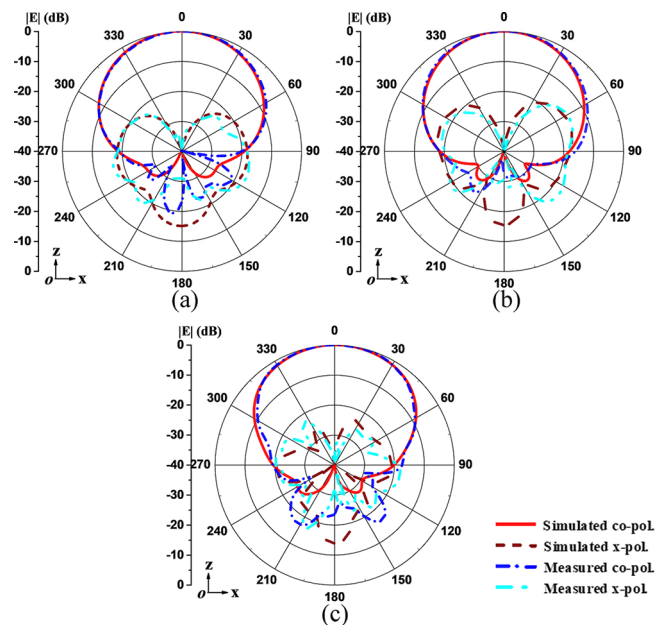


Figure 25. Radiation patterns of the bandwidth-enhanced broadband antenna for $+45^\circ$ polarization at (a) 1.4 GHz, (b) 2.2 GHz, and (c) 2.7 GHz.

Fig. 20. The bandwidth-enhanced broadband antenna is designed to cover the 2 GHz band (1.7–2.7 GHz) for 2G/3G/4G systems

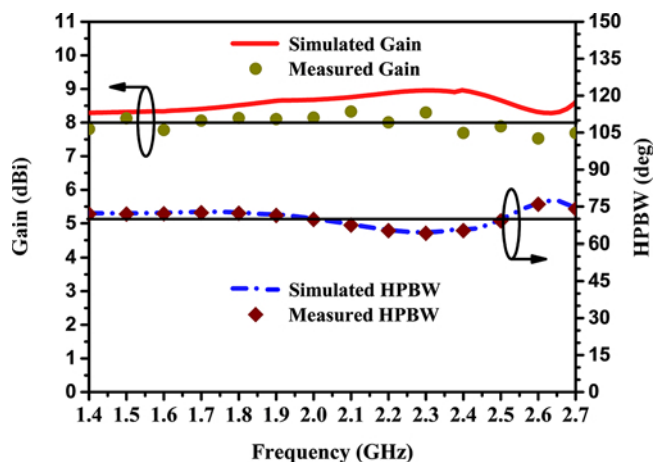


Figure 26. Gain and HPBW of the bandwidth-enhanced broadband antenna.

Table 1. Comparison of this work with published literature.

Reference	Bandwidth (%)	Geometric parameters	Antenna complexity
[2]	44 (VSMR > 1)	8	Moderate
[3]	45 (RL > 15 dB)	7	Moderate
[4]	45 (VSMR < 1.5)	8	Moderate
[5]	57.7 (VSMR < 1.5)	22	Complex
[6]	52 (VSMR < 1.5)	18	Complex
[7]	51 (RL > 15 dB)	19	Complex
[8]	56.5 (VSMR < 1.5)	23	Complex
[9]	67 (RL > 15 dB)	16	Complex
[10]	67.3 (VSMR < 1.5)	25	Complex
[11]	61 (VSMR < 1.5)	10	Moderate
[12]	63 (VSMR < 1.5)	34	Complex
[13]	64.7 (VSMR < 1.5)	17	Complex
This work	50 (RL > 15 dB)	3	Simple
Ant.I			
This work	67 (RL > 15 dB)	6	Simple
Ant.II			

and the 1427–1518 MHz band for international mobile telecommunications (IMT) services. Three new geometric parameters are involved in the design of the bandwidth-enhanced broadband antenna, including the slot lengths (L_1 and L_2) and the slot width (w). The third resonance is created by the introduction of the slots at f_{r3} , as shown in Fig. 21, thus resulting in a bandwidth enhancement. Each dipole of the bandwidth-enhanced broadband antenna acts at f_{r3} as a top-loaded half-wave dipole, as suggested by the current distribution displayed in Fig. 22.

A prototype of the bandwidth-enhanced broadband antenna is presented in Fig. 23. The simulated and measured S-parameters are plotted in Fig. 24. The measured bandwidth for RL > 15 is about 67% (1.39–2.71 GHz), covering the frequency band for 2G/3G/4G systems and IMT services. The measured isolation is higher than 35 dB for most parts of the frequency band. The radiation patterns simulated and measured at 1.4, 2.2, and 2.7 GHz are plotted in

Fig. 25; stable radiation patterns are observed. The gain and the HPBW of the bandwidth-enhanced broadband antenna are presented in Fig. 26. The measured antenna gain is about 8 ± 0.5 dBi and the HPBW is $70 \pm 5^\circ$.

A comparison of the broadband antennas developed in this work with those published in literature in terms of bandwidth (BW), the number of geometric parameters involved (not including the ground plane), and antenna complexity is presented in Table 1. For a bandwidth of ~45%, the dual-polarized antennas proposed in [2–4] have used 7–8 geometric parameters, while the design of the broadband antenna (Ant. I) in this work has only 3 geometry parameters involved. The bandwidth-enhanced broadband antennas presented in [5–13] adopted a variety of numbers of geometry parameters from 10 to 34, while the bandwidth-enhanced broadband antenna (Ant. II) in this work only needs 6 geometric parameters. Both broadband antennas developed in this work feature a simple planar configuration, high isolation, and stable radiation patterns.

Conclusion

A simple procedure for the design of broadband planar base station antennas is presented. Based on a square patch, a bandwidth of 50% for RL > 15 dB is realized by adjusting two critical geometric parameters for a broadband antenna. The bandwidth of the broadband antenna is enhanced to 67% for RL > 15 dB by introducing four Γ slots into the broadband antenna and optimizing five geometric parameters. Both broadband antennas feature a simple planar configuration, high isolation, and stable radiation patterns with a realized gain of about 8 ± 0.5 dBi and a HPBW of $70 \pm 5^\circ$.

Acknowledgements. This work was supported in part by the National Natural Science Foundation of China (grant 62071185) and in part by the Natural Science Foundation of Guangdong Province (2021A1515011993).

Competing interests. The authors report no conflicts of interest.

References

- R-S Chen, G-L Huang, S-W Wong, MKT Al-Nuaimi, K-W Tam and W-W Choi (2023) Bandwidth-enhanced circularly polarized slot antenna and array under two pairs of degenerate modes in a single resonant cavity. *IEEE Antennas and Wireless Propagation Letters* **22**, 288–292.
- Y Liu, H Yi, F-W Wang and S-X Gong (2013) A novel miniaturized broadband dual-polarized dipole antenna for base station. *IEEE Antennas and Wireless Propagation Letters* **12**, 1335–1338.
- Y-H Cui, R-L Li and H-Z Fu (2014) A broadband dual-polarized planar antenna for 2G/3G/LTE base stations. *IEEE Transactions on Antennas and Propagation* **62**, 4836–4840.
- L-H Wen, S Gao, Q Luo, C-X Mao, W Hu, Y-Z Yin, Y-G Zhou and Q-W Wang (2018) Compact dual-polarized shared-dipole antennas for base station applications. *IEEE Transactions on Antennas and Propagation* **66**, 6826–6834.
- Z-D Bao, Z-P Nie and X-Z Zong (2014) A novel broadband dual-polarization antenna utilizing strong mutual coupling. *IEEE Transactions on Antennas and Propagation* **62**, 450–454.
- Y-S Gou, S-W Yang, J-X Li and Z-P Nie (2014) A compact dual-polarized printed dipole antenna with high isolation for wideband base station applications. *IEEE Transactions on Antennas and Propagation* **62**, 4392–4395.
- D-Z Zheng and Q-X Chu (2017) A multimode wideband $\pm 45^\circ$ dual-polarized antenna with embedded loops. *IEEE Antennas and Wireless Propagation Letters* **16**, 633–636.
- Y-Z Chen, W-B Lin, S Li and A Raza (2018) A broadband $\pm 45^\circ$ dual-polarized multidipole antenna fed by capacitive coupling. *IEEE Transactions on Antennas and Propagation* **66** 2644–2649.

9. L-J Wu, R-L Li, Y Qin and Y-H Cui (2018) Bandwidth-enhanced broadband dual-polarized antennas for 2G/3G/4G and IMT services. *IEEE Antennas and Wireless Propagation Letters* **17**, 1702–1706.
10. S-D Fu, Z-X Cao, P Chen, D Gao and X Quan (2019) A novel bandwidth-enhanced dual-polarized antenna with symmetrical closed-resonant-slot pairs. *IEEE Access* **7**, 87943–87950.
11. L-H Wen, S Gao, Q Luo, Q-L Yang, W Hu, Y-Z Yin, X-F Ren and J Wu (2019) A compact wideband dual-polarized antenna with enhanced upper out-of-band suppression. *IEEE Transactions on Antennas and Propagation* **67**, 5194–5202.
12. C-F Ding, X-Y Zhang and M Yu (2020) Simple dual-polarized filtering antenna with enhanced bandwidth for base station applications. *IEEE Transactions on Antennas and Propagation* **68**, 4354–4361.
13. L-H Ye, X-Y Zhang, Y Gao and Q Xue (2020) Wideband dual-polarized four-folded-dipole antenna array with stable radiation pattern for base-station applications. *IEEE Transactions on Antennas and Propagation* **68**, 4428–4436.
14. KM Mak, HW Lai and KM Luk (2018) A 5G wideband patch antenna with antisymmetric L-shaped probe feeds. *IEEE Transactions on Antennas and Propagation* **66**, 957–961.
15. L-H Wen, S Gao, Q Luo, W Hu, Q-L Yang, Y-Z Yin, X-F Ren and J Wu (2019) A wideband differentially driven dual-polarized antenna by using integrated six-port power divider. *IEEE Transactions on Antennas and Propagation* **67**, 7252–7260.
16. Z-Y Tang, J-H Liu, R Lian, Y-P Li and Y-Z Yin (2019) Wideband differentially fed dual-polarized planar antenna and its array with high common-mode suppression. *IEEE Transactions on Antennas and Propagation* **67**, 131–139.